velocity affects the temperature through the kinetic energy, and since the calculated streamwise velocity is too large, the kinetic energy is too large, resulting in a lower than correct value of the peak temperature in the boundary layer.

The error in predicting the peak temperature may not appear catastrophic because of the good prediction of the wall heat transfer. However, parabolized methods are important for the calculation of reacting flowfields with finite reaction rates.[8] The reaction rates are usually modeled as an exponential function of temperature. Therefore, a minor discrepancy in the temperature can result in a gross error in the species concentrations.

Adiabatic Wall with Linear Viscosity Law

To evaluate the error made in skin friction, the flow over a flat plate has been computed for an adiabatic wall with a linear viscosity law instead of Sutherland's equation:

$$\frac{\mu}{\mu_0} = \frac{T}{T_0} \tag{6}$$

For this case the solution of the boundary-layer equations results in a local coefficient of skin friction that is independent of Mach number and is[9]

$$C_f = \frac{0.664}{\sqrt{Re_x}} \tag{7}$$

Solutions to the PNS equations were computed for Mach numbers 2, 4, 6, and 8, with and without the correction terms, using the finite difference code. Each case was run on a fixed grid and continued downstream until the local value of $C_f\sqrt{Re_x}$ approached its asymptotic limit, signaling the end of the weak interaction region. The difference between the corrected PNS solution and the boundary-layer solution is $<3\%$, whereas the PNS uncorrected solution resulted in a difference of up to 42% (Fig. 4). The difference between the boundary-layer solution and the uncorrected PNS solution is clearly unreasonable.

Concluding Remarks

A source of error in the implementation of Vigneron's technique with fully conservative differencing has been identified and explained by a force balance analysis. Significant errors in the skin-friction coefficient and the maximum temperature in boundary-layer profiles have been demonstrated in numerical solutions of supersonic flow over a flat plate. This type of error has a special significance in computational fluid dynamics codes that use finite rate chemical reactions since the maximum temperature controls the chemical reactions. In addition, these numerical solutions have been shown to be dependent on the grid topology. The proposed procedure eliminates these problems.

Acknowledgments

The work of the first author was supported under NASA Contract NAS1-18599. The authors thank A. Douglas Dilley for providing the boundary-layer solutions.

References

[1]Vigneron, Y. C., Rakich, J. V., and Tannehill, J. C., "Calculation of Supersonic Viscous Flow over Delta Wings with Sharp Subsonic Leading Edges," AIAA Paper 78-1137, July 1978.

[2]Newsome, R. W., Walters, R. W., and Thomas, J. L., "An Efficient Iteration Strategy for Upwind/Relaxation Solutions to the Thin-Layer Navier-Stokes Equations," AIAA Paper 87-1113, June 1987.

[3]Gielda, T. P., and McRae, D. S., "An Accurate, Stable, Explicit, Parabolized Navier-Stokes Solver for High-Speed Flows," AIAA Paper 86-1116, May 1986.

[4]Korte, J. J., "An Explicit Upwind Algorithm for Solving the Parabolized Navier-Stokes Equations," NASA TP 3050, Feb. 1991.

[5]Morrison, J. H., and Korte, J. J., "Implementation of Vigneron's Streamwise Pressure Gradient Approximation in the PNS Equations," AIAA Paper 92-0189, Jan. 1992.

[6]Lawrence, S. L., Tannehill, J. C., and Chaussee, D. S., "An Upwind Algorithm for the Parabolized Navier-Stokes Equations," AIAA Paper 86-1117, May 1986.

[7]Harris, J. E., and Blanchard, D. K., "Computer Program for Solving Laminar, Transitional, or Turbulent Compressible Boundary-Layer Equations for Two-Dimensional and Axisymmetric Flow," NASA TM 83207, Feb. 1982.

[8]Kamath, H., "Parabolized Navier-Stokes Algorithm for Chemically Reacting Flows," AIAA Paper 89-0386, Jan. 1989.

[9]Schlichting, H., *Boundary-Layer Theory*, 7th ed., McGraw-Hill, New York, 1979, p. 337.

Gaster's Transform

A. P. Roychowdhury* and B. N. Sreedhar†
Indian Institute of Technology, Kharagpur, Pin, 721302 India

I. Introduction

GASTER[1] proposed a transformation to convert the temporally growing disturbances into spatial growth rates by connecting them using group velocity, for application to hydrodynamic stability analysis. Before the development of this transform, Schubauer and Skramskad,[2] Sato,[3] and others used phase velocity as the connecting parameter between spatial and temporal amplification rates of disturbances. Freymuth[4] experimentally established the need for the use of spatial growth rates to predict the stability characteristics of free shear layer flows. Gill,[5] Michalke,[6] Gaster,[7] and Mack[8] also used the spatial growth rates in the study of stability characteristics of both incompressible and compressible flows.

Though Gaster[1] has clearly indicated that his transformation was valid for small growth rates of disturbances only, he did not explicitly indicate the range. This has led to the failure of Gaster's transformation in the prediction of the spatial growth rates when used outside the range of its applicability. Direct numerical evaluation of spatial growth rates obtained on solving the linear stability eigenvalue problem and the experimental data have shown poor comparison with spatial growth rates obtained from temporal calculations using Gaster's transformation.

This Note addresses this question of why such a discrepancy exists in the values predicted using Gaster's transformation. The transformation will be shown to be valid only very close to the neutral point corresponding to $\alpha_r = 0$ and $\alpha_i = 0$, where α is complex and represents the normal mode of decomposition of the disturbance field.

II. Derivation of Gaster's Transform

A geometric point of view will be used to highlight some of the assumptions that are not explicitly indicated by Gaster[1] in his proof that might have led to the application of the transformation outside the range of its applicability. If α = wave number, ω = wave frequency, and c = phase speed, in temporal analysis, it is assumed that $\alpha = \alpha_r$ is real, $\omega = \omega_r + i\omega_i$ and $c = c_i + ic_i$ are complex, $c_i\alpha$ is the temporal amplification rate; and in the spatial stability analysis, $c = c_r$ is real, $\omega = c\alpha = c_r\alpha_r + ic_i\alpha_i = \omega_r + i\omega_i$ is complex, and $\omega_i = \alpha_i c_r$ is the spatial amplification rate.

Received Nov. 4, 1991; revision received Dec. 9, 1992; accepted for publication Dec. 18, 1991. Copyright © 1992 by the American Institute of Aeronautics and Astronautics, Inc. All rights reserved.

*Research Scholar, Department of Aerospace Engineering. Member AIAA.

†Professor and Head, Department of Aerospace Engineering.

The group velocity is different in the spatial and the temporal framework mainly because the phase velocity is different in the spatial framework when compared with its value in the temporal framework. The fluid being a dispersive medium, the group velocity may be defined using Brillouin's equation,

$$c_g = c_{ph} + \frac{\alpha \partial(c_{ph})}{\partial \alpha} = \frac{\partial \omega}{\partial \alpha}$$

where c_g and c_{ph} are the group and phase velocities, respectively.

On assuming ω is analytic in the complex α plane, the Cauchy Riemann condition yields the following two equations:

$$\frac{(\partial \omega_r)_{\alpha_i}}{\partial \alpha_r} = \frac{(\partial \omega_i)_{\alpha_r}}{\partial \alpha_i} \tag{1a}$$

$$\frac{(\partial \omega_r)_{\alpha_r}}{\partial \alpha_i} = -\frac{(\partial \omega_i)_{\alpha_i}}{\partial \alpha_r} \tag{1b}$$

The neutral point corresponds to $\alpha_r = \alpha_i = 0$. The spatial group velocity is $\partial\omega/\partial\alpha$. Close to the neutral point corresponding to $\alpha_r = \alpha_i = 0$, $c_g = (\partial\omega_r)_{\alpha_i=0}/\partial\alpha_r$ (since $\alpha_i \Rightarrow 0$ defines a neutral point). Also the temporal group velocity is given by $\partial\omega/\partial\alpha$.

Hence, close to the neutral point (Fig. 1) corresponding to $\alpha_r = \alpha_i = 0$, $\omega = \omega_r + i\omega_i = \alpha_r(c_r + ic_i) = \alpha_r c_r = \omega_r$ (since $c_i \Rightarrow 0$ defines a neutral point). Thus, $[\partial\omega_r/\partial\alpha_r]_{\alpha_i=0} = c_g(T)$. Hence, it is seen that, for a point very close to the neutral point corresponding to $\alpha_r = \alpha_i = 0$,

$$\left[\frac{\partial \omega_r}{\partial \alpha_r}\right]_{\alpha_i = 0} = c_g(T) = \text{temporal group velocity at } T$$

$$= \text{spatial group velocity at } S$$

provided, of course, that the points T and S lie in the neighborhood of the neutral point corresponding to $\alpha_r = \alpha_i = 0$. Further, using the Cauchy Riemann condition given in Eq. (1a), one gets

$$\left[\frac{\partial \omega_r}{\partial \alpha_r}\right]_{\alpha_i = 0} = \left[\frac{\partial \omega_i}{\partial \alpha_i}\right]_{\alpha_r = 0} = c_g$$

$$\left[\frac{\partial \omega_i}{\partial \alpha_i}\right]_{\alpha_r = 0} = \lim_{\alpha_r \Rightarrow 0} \Delta\omega_i/\Delta\alpha_i \tag{2}$$

$$= \lim_{\alpha_r \to 0} [\omega_i(S) - \omega_i(T)]/[\alpha_i(S) - \alpha_i(T)]$$

Recall that $\omega_i(S) = \alpha_i c_r$ and $\omega_i(T) = \alpha_r c_i$. Also it is seen that $\omega_i(T) \Rightarrow 0$ since $\alpha_r \Rightarrow 0$ at point T and $\alpha_i(T) \Rightarrow 0$ because any temporal disturbance has a real wave number. Hence,

$$\left[\frac{\partial \omega_i}{\partial \alpha_i}\right]_{\alpha_r = 0} = c_g = \lim_{\alpha_r \to 0} \frac{\omega_i(S)}{\alpha_i(S)}$$

On expanding $\omega_i(S)$ about the point T (the distance between the points S and T is geometrically equal to α_i), one gets

$$\omega_i(S) = \omega_i(T) + \left[\frac{\partial \omega_i}{\partial \alpha_r}\right]_{\alpha_i = 0} + \left[\frac{\partial^2 \omega_i}{\partial \alpha_r^2}\right]_T (\alpha_i^2)$$

$$+ \text{higher order terms} \tag{3}$$

Gaster[1] has used the fact that $(\partial\omega_i/\partial\alpha_r) \sim 0(\omega_{im})$ (where ω_{im} corresponds to the maximum of ω_i). He had used the data from the experiments of Shen[9] (for Poiseuille and Blausius flow) to show that $\omega_{im} \approx 10^{-3}$. Adopting this information from Gaster's work[1] in this analysis too, one sees that second-order terms can be neglected in Eq. (3) [because α_i is small and $(\partial\omega_i/\partial\alpha_r)$, α_i is also a small quantity of order 10^{-4} and smaller], and one has $\omega_i(S) = \omega_i(T)$ for S and T close to the neutral point corresponding to $\alpha_r = \alpha_i = 0$. Hence,

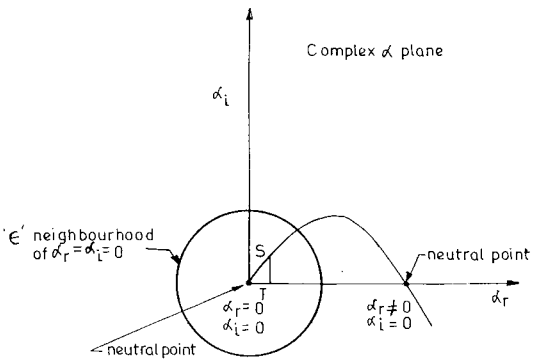

Fig. 1 Neutral points in the complex α plane.

$$c_g = \lim_{\alpha_r \to 0} \omega_i(T)/\alpha_i(S) = \omega_i(T)/\alpha_i(S) \tag{4}$$

Gaster[1] had used a similar hypothesis to prove that

$$\frac{\partial \omega_r}{\partial \alpha_r} = -\frac{\omega_i(T)}{\alpha_i(S)} \tag{5}$$

which is valid for small rates of amplifications. However, not emphasized by Gaster[1] was the condition under which $(\partial\omega_r/\partial\alpha_r)$ could be equated to the group velocity c_g. The considerations that the group velocity c_g is equal to $(\partial\omega_r/\partial\alpha_r)$ only in the neighborhood of the neutral point where $\alpha_r = \alpha_i = 0$ are not categorically stated in his proof. Further, the spatial and temporal values of the group velocity that are equal to each other in the neighborhood of this neutral point corresponding to the origin of the complex wave number space, which is another speciality of this neutral point, have not been mentioned in his proof. Hence, the failure of Gaster's transformation in converting temporal to spatial growth rates is caused by the fact that this transformation has a very strict requirement that the values of α_r and α_i should be close to zero. In other words, the requirement set forth by Gaster[1] that the growth rates, both temporal and spatial, should be small is not enough; in fact the growth rates should be very small. Hence, the range of applicability of Gaster's transform in predicting spatial growth rates from temporal growth rates is a very small one.

In the next section some numerical calculations of spatial and temporal growth rates are presented so as to allow one to determine the validity of Gaster's transformation very close to the $\alpha_r = \alpha_i = 0$ neutral point and for those points far away from it.

III. Results and Discussions

The inviscid form of the linear stability equation for an incompressible isothermal fluid is solved. After incorporating parallel flow assumption and normal mode decomposition, the linear disturbance equation is solved for the unbounded case using the consistent boundary conditions. For temporal calculation, the value of α is taken as complex and that of c as real and vice versa for the spatial case. The results are tabulated in Table 1. The calculations using Gaster's transformation are compared directly with those obtained from spatial calculations. This has been done for a cluster of points close to $\alpha_r = \alpha_i = 0$ and α_r and $\alpha_i = 0$. The mean velocity profiles are 1) $U_0 = 1 + \tanh z$ and 2) $U_0 = \text{sech}^2 z$, representing a mixing layer and a jet, respectively.

It is noticed that for both the mixing layer and the jet case, computations using incompressible considerations show that the estimates of spatial growth rates obtained from temporal calculations using Gaster's transformation when compared

Table 1 Comparison of the spatial growth rates obtained from temporal calculations using Gaster's transformation with those obtained from direct spatial calculations

Temporal calculations	α	c		ω		c_g		Gaster's transformation value, α_i
		c_r	c_i	ω_r	ω_i	c_{g_r}	c_{g_i}	
Incompressible case								
Mixing layer, $U_0 + 1 \tanh z$								
Close to $\alpha_r = \alpha_i = 0$	0.001	1.0	5.0e−4	0.001	5.0e−7	2.0	2.0e−5	0.025
	0.002	1.0	1.0e−5	0.002	2.0e−8			
	0.003	1.0	5.0e−6	0.003	1.5e−8			
	0.004	1.0	1.0e−6	0.004	4.0e−9			
Away from $\alpha_r + \alpha_i = 0$	0.1	1.0	1.0e−7	0.1	1.0e−8	2.0	2.0e−7	0.05
	0.2	1.0	1.0e−7	0.2	2.0e−8			
	0.3	1.0	1.0e−7	0.3	3.0e−8			
	0.4	1.0	1.0e−8	0.4	4.0e−9			
Jet $U_0 = \text{sech}^2 z$								
Close to $\alpha_r = \alpha_i = 0$	0.001	1.0	1.0e−5	1.0e−3	1.0e−8	2.0	1.0e−5	0.001
	0.002	1.0	5.0e−6	2.0e−3	1.0e−8			
	0.003	1.0	1.0e−7	3.0e−3	3.0e−10			
	0.004	1.0	5.0e−8	4.0e−3	2.0e−10			
Away from $\alpha_r = \alpha_i = 0$	0.1	1.0	1.0e−13	1.0e−1	1.0e−14	2.0	−1.0e−13	−0.1
	0.15	1.0	1.0e−15	1.5e−1	1.0e−16			
	0.20	1.0	1.0e−14	2.0e−1	2.0e−15			
	0.25	1.0	1.0e−13	2.5e−1	1.5e−15			

Spatial calculations	α		c		ω		Difference in phase velocity, %
	α_r	α_i	c_r	c_i	ω_r	ω_i	
Incompressible case							
Mixing layer, $U_0 = 1 + \tanh z$							
Close to $\alpha_r = \alpha_i = 0$	0.001	0.025	1.0	5.0e−4	9.875e−4	0.025	0
	0.002						
	0.003						
	0.004						
Away from $\alpha_r = \alpha_i = 0$	0.1	0.05	1.0	0.5	0.075	0.1	50
	0.2						
	0.3						
	0.4						
Jet $U_0 = \text{sech}^2 z$							
Close to $\alpha_r = \alpha_i = 0$	0.001	0.001	1.0	1.0e−5	0.001	0.001	0
	0.002						
	0.003						
	0.004						
Away from $\alpha_r = \alpha_i = 0$	0.1	−0.1	1.5	0.5	0.2	−0.1	70.7
	0.15						
	0.20						
	0.25						

with direct spatial evaluation show differences of less than 1% (at most instances it is close to 0%) for α_r and α_i very close to zero. For larger values of α, even as small as 0.1, errors up to 71% are noticed. Table 1 should be referred to for such a comparison. These calculations are done for the jet profile.

IV. Conclusions

From the numerical results one obtains the basis for the confident conclusion that the applicability of Gaster's transformation[1] is very much limited to the region in the ϵ neighborhood of the neutral point corresponding to $\alpha(\alpha_r, \alpha_i) = (0,0)$ (the limit of ϵ is zero). Gaster's analysis[1] states that the transformation is limited to small growth rates, which however did not specify the domain over which it is valid. The present analysis, therefore, would be a better indication to researchers in this area about the cause of such a failure.

References

[1]Gaster, M., "A Note on the Relation Between Temporally Increasing Disturbances in Hydrodynamic Stability," *Journal of Fluid Mechanics*, Vol. 14, No. 2, 1962, pp. 222–224.

[2]Schubauer, G. B., and Skramskad, H. K., "Laminar Boundary Oscillations and Transition on a Flat Plate," *Journal of the Aeronautical Sciences*, Vol. 14, No. 1, 1947, pp. 69–78.

[3]Sato, H., "Experimental Investigation of the Transition of Laminar Separated Flows," *Journal of the Physical Society of Japan*, Vol. 11, No. 6, 1956, pp. 702–709.

[4]Freymuth, P., "On Transition in a Separated Laminar Boundary Layer," *Journal of Fluid Mechanics*, Vol. 25, No. 4, 1966, pp. 683–704.

[5]Gill, A. E., "Instabilities of 'Top-Hat' Jets and Wakes in Compressible Flows," *Physics of Fluids*, Vol. 8, No. 8, 1965, pp. 1428–1430.

[6]Michalke, A., "On Spatially Growing Disturbances in an Inviscid Shear Layer," *Journal of Fluid Mechanics*, Vol. 23, No. 3, 1965, pp. 521–544.

[7]Gaster, M., "On the Generation of Spatially Growing Waves in a Boundary Layer," *Journal of Fluid Mechanics*, Vol. 22, No. 3, 1965, pp. 433–441.

[8]Mack, L. M., "Boundary Layer Stability," Jet Propulsion Lab., California Inst. of Technology, Rept. 900-277, Rev. A, Pasadena, CA, 1969.

[9]Shen, S. F., "Calculated Damped Oscillations in Plane Poiseuille and Blasius Flows," *Journal of the Aeronautical Sciences*, Vol. 21, No. 1, 1954, pp. 62–64.